Discontinuous Galerkin Time Domain Method with Dispersive Modified Debye Model and its Application to the Analysis of Optical Frequency Selective Surfaces

Wending Mai, Benjamin Zerbe, and Douglas H. Werner

The Pennsylvania State University, University Park, PA 16802 USA
wdmai@psu.edu, baz5128@psu.edu, dhw@psu.edu

Abstract **─** We develop a discontinuous Galerkin time domain (DGTD) algorithm with an experimentally validated modified Debye model (MDM) to take metal dispersion into consideration. The MDM equation is coupled with Maxwell's equations and solved together through the auxiliary differential equation (ADE) method. A Runge-Kutta time-stepping scheme is proposed to update the semi-discrete transformed Maxwell's equations and ADEs with high order accuracy. Then we employ the proposed algorithm to analyze an infinite doubly periodic frequency selective surface (FSS) operating in the optical regime that exhibits transmission enhancement due to the surface plasmatic effect. The accuracy and the efficiency enhancements are validated through a comparison with commercial simulation software. This work represents the first integration of MDM with DGTD, which enables the DGTD algorithm to efficiently analyze metallic structures in the optical regime.

Index Terms **─** Auxiliary Differential Equation (ADE) method, Discontinuous Galerkin Time Domain (DGTD), Frequency Selective Surface (FSS), Modified Debye Model (MDM), prism elements.

I. INTRODUCTION

The necessity of handling dispersive media is important to several applications. For example, applications in optical electromagnetic wave therapy, imaging, and bio-electromagnetic hazards require the simulation of waves in biological tissues that are inherently dispersive. Similarly, undersea and underground penetrating radar applications assume geological media that are also inherently dispersive. Optical or terahertz frequency selective surfaces (FSS) [1]–[3], electromagnetic band gap (EBG) structures [4], and engineered materials (*e.g.*, metamaterials) [5]–[9] are also inherently dispersive. These structures, which are comprised of a repeating metallic pattern, have a wide range of applications in electromagnetic and optical engineering. Several closed form mathematical models have been proposed to represent material dispersion properties. For example, researchers have used the Debye model to simulate the relaxation property, the Lorentz model to represent the resonance process, and the Drude model to take into consideration cold-plasma features. Moreover, the auxiliary differential equation method (ADE) was proposed to circumvent the time-consuming convolution operation. It was originally introduced in conjunction with the finite difference time domain (FDTD) technique [10], [11], and then also implemented in FETD [12] and DGTD [13] methods. The DGTD technique has become the subject of much attention due to its high degree of accuracy, which stems from flexible meshing and high order basis functions. Moreover, it is efficient because of its suitability for element-wise parallelization. More recently, a combination of different models, namely the generalized dispersion model (GDM), was incorporated into DGTD to facilitate full wave simulation of dispersive materials [14]-[22].

The conventional Debye model is widely used to model dispersive dielectric materials in the microwave regime. However, it cannot accurately represent metals that are dispersive in the optical regime. By adding an extra conductivity term, the modified Debye model (MDM) has been used in the FDTD method to model dispersive metals in the optical regime [10], [11]. With the additional conductive term, the degree of freedom of MDM is the same as the Drude model. Therefore, research shows that these two models can be viewed as mathematically equivalent. The MDM model is capable of representing Drude-like metals in the optical regime, while keeping the simplicity of the Debye model. Therefore, it can be easily adapted by researchers familiar with microwave Debye materials to explore the dispersive properties in the optical regime. Many studies have been performed to determine the optimal parameter settings for MDM that accurately fit experimental data over a broad frequency band [23]–[25]. However, there has apparently been no prior work done to incorporate MDM with DGTD to facilitate the efficient modeling of

Submitted On: August 4, 2020
Accepted On: December 10, 2020
https://doi.org/10.47037/2020.ACES.J.360104

dispersive metals.

This paper presents the first integration of the MDM and DGTD methods. It enables a prism-based DGTD algorithm to efficiently analyze dispersive planar metallic structures in the optical regime. A frequency selective surface (FSS) composed of a gold film with a periodic array of air holes was analyzed to validate the accuracy and efficiency of the proposed algorithm. In Section II, the prism-based DGTD method with the MDM is presented. A numerical example is shown in Section III to validate the accuracy and efficiency improvement of the proposed method.

II. FORMULATION

In order to take into account the material dispersion of metal in the optical spectrum, researchers have collected experimental data. In order to fit the measured data, and to conduct associated time-domain simulations, various methods have been proposed. Krug *et al.* have attempted to extract gold parameters in the near-infrared range. But their results deviate significantly from accepted experimental values [23]. Jin *et al.* have recently determined gold parameters applicable in the wavelength range 550–950 nm [24]. More recently, Gai et al proposed a series of modified Debye model parameters for metals that are applicable for broadband calculations [25]. The conventional Debye model was modified by adding an extra conductivity term to better represent metal's dispersive performance at optical frequencies:

$$\varepsilon_{\mathrm{r}} = \varepsilon_\infty + \frac{\varepsilon_s-\varepsilon_\infty}{1+i\omega\tau} + \frac{\sigma}{i\omega\varepsilon_0}, \qquad (1)$$

where ε_{r} is the complex relative permittivity, ε_s and ε_∞ are the zero-frequency (static) and infinite-frequency relative permittivity values, respectively. ω is the angular frequency, while the component $i\omega$ in the frequency domain represents the engineering convention corresponding to time-varying fields as $e^{i\omega t}$. Here ε_0 is the permittivity of free space, τ is the relaxation time, and σ is the introduced conductivity. We should also note that Eq. (1) represents a purely mathematical model and, therefore, is not based on any physical description of separating bound charges and free charges or the associate currents [26].

Figure 1 demonstrates the material dispersion of gold as determined from experimental measurements and from the modified Debye fitting model. The parameters of the model are set as: $\varepsilon_s = -15789$, $\varepsilon_\infty = 11.575$, $\sigma = 1.6062 \times 10^7\ S/m$, and $\tau = 8.71 \times 10^{-15} s$ [25]. As shown in Fig. 1, both the real and the imaginary parts of the modified Debye model permittivity agree well with those obtained from the measurements [27]. Hence, it can be concluded that the modified Debye model with the indicated parameters is accurate over a broad frequency band: 250 THz to 428 THz. The bandwidth of the model spectrum is limited physically by the existence of inter-band transitions, which are not accounted for in the MDM.

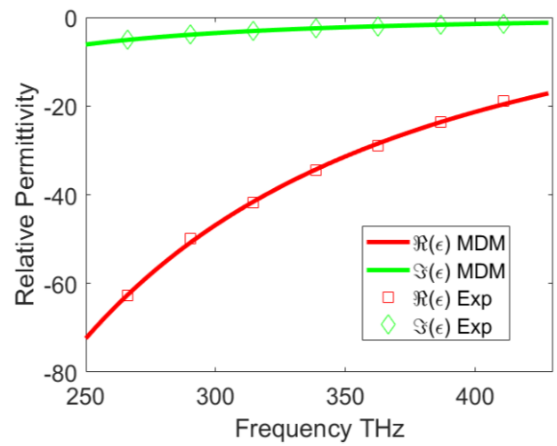

Fig. 1. Comparison between the relative permittivity of gold from the modified Debye model (MDM) and from experimentally determined results (Exp) [27].

Previously, the modified Debye model has been incorporated into the FDTD method [10]–[11], [25]. In this work, and for the first time, we integrated the modified Debye model with DGTD for accurate and efficient computation of dispersive material systems.

By considering the displacement current $\overrightarrow{J_D} = i\omega\vec{D}$, the conductivity in (1) can be incorporated into Ampere's equation with the MDM term:

$$\nabla \times \vec{\boldsymbol{H}} = \sigma\vec{\boldsymbol{E}} + i\omega\varepsilon_0\varepsilon_\infty\vec{E} + \overrightarrow{\boldsymbol{J_p}}, \qquad (2)$$

where $\vec{\boldsymbol{E}}$ and $\vec{\boldsymbol{H}}$ represent the frequency domain (bold) electric and magnetic field vectors, respectively, while the introduced polarization current vector $\overrightarrow{\boldsymbol{J_p}}$ is defined as:

$$\overrightarrow{\boldsymbol{J_p}} = i\omega\varepsilon_0\left(\frac{\varepsilon_s-\varepsilon_\infty}{1+i\omega\tau}\right)\vec{E}. \qquad (3)$$

Through application of an inverse Fourier transformation, (3) can be recast in the form of an auxiliary differential equation (ADE):

$$\frac{d\overrightarrow{J_p}}{dt} = \frac{\varepsilon_0(\varepsilon_s-\varepsilon_\infty)}{\tau}\frac{d\vec{E}}{dt} - \frac{\overrightarrow{J_p}}{\tau} \qquad (4)$$

Here, the ADE in (4) only contains a first-order time derivative term. Solving this is more efficient than for models with higher order time derivative terms.

Accordingly, the dispersive form of Maxwell's curl equations can be transformed into the time domain as:

$$\mu_r\mu_0\frac{d\vec{H}}{dt} = -\nabla \times \vec{E}, \qquad (5)$$

$$\sigma\vec{E} + \varepsilon_r\varepsilon_0\frac{d\vec{E}}{dt} + \overrightarrow{J_p} = \nabla \times \vec{H}, \qquad (6)$$

where $\vec{E}$, $\vec{H}$, and $\overrightarrow{J_p}$ are the electric, magnetic and polarization vectors in the time domain (unbold).

Suppose that the computational domain is split into N non-overlapping prismatic elements Ω_m, where the electric and magnetic fields, as well as the electric polarization vector are expanded by the basis functions $\vec{\Phi}_k^i(r)$:

$$\overrightarrow{E^m}(r,t) = \sum_{l=1}^{N_e^m} e_l^m(t)\vec{\Phi}_l^m(r), \quad (7)$$

$$\overrightarrow{H^m}(r,t) = \sum_{l=1}^{N_h^m} h_l^m(t)\vec{\Phi}_l^m(r), \quad (8)$$

$$\overrightarrow{J_p^m}(r,t) = \sum_{l=1}^{N_j^i} j_l^m(t)\vec{\Phi}_l^m(r), \quad (9)$$

where N_e^m, N_h^m, and N_j^m represent the number of basis functions for $\vec{E}$, $\vec{H}$ and $\overrightarrow{J_p}$ in element m, respectively.

The integration of the DGTD method and the MDM outlined in the previous section is independent of the element type. But for planar structures such as FSS and metasurfaces, it is more optimal to discretize them into triangular prisms instead of conventional tetrahedrons. The prismatic discretization of space will not only reduce the element number, but also improve the mesh quality, which is often problematic for a tetrahedral-based mesh when dealing with very thin layer structures.

To model the curl operator in Maxwell's equations, we introduce a numerical upwind flux that is based on the Rankine Hugoniot jump relations. Then, by performing Galerkin testing over Maxwell equations, and taking into account the numerical flux and MDM term, we obtain the following DGTD semi-discretized matrix equations:

$$\frac{de^m}{dt} = \frac{1}{\varepsilon_0\varepsilon_\infty}\{\bar{M}_e^{m-1}\cdot\Big[\bar{S}_e^m h^m + \sum_{f=1}^{N_m^f}\big(\bar{F}_{ee}^{mm,f}e_f^m + \bar{F}_{ee}^{mn,f}e_f^n + \bar{F}_{eh}^{mm,f}h_f^m + \bar{F}_{eh}^{mn,f}h_f^n\big) + \beta\cdot\bar{F}_e^{m,M_s}\Big] - \sigma e^m - \varepsilon_0 j^m\}, \quad (10)$$

$$\frac{dh^m}{dt} = \bar{M}_h^{m-1}/\mu_0\mu_{\mathrm{r}}\cdot\Big[-\bar{S}_h^m e^m + \sum_{f=1}^{N_m^f}\big(\bar{F}_{hh}^{mm,f}h_f^m + \bar{F}_{hh}^{mn,f}h_f^n + \bar{F}_{he}^{mm,f}e_f^m + \bar{F}_{he}^{mn,f}e_f^n\big) + \beta\cdot\bar{F}_h^{m,M_s}\Big], \quad (11)$$

$$\frac{dp^m}{dt} = \frac{(\varepsilon_s-\varepsilon_\infty)}{\tau}\frac{de^m}{dt} - \frac{j^m}{\tau}, \quad (12)$$

where $\bar{M}, \bar{S},$ and $\bar{F}$ denote the mass matrix, the stiffness matrix and the flux matrix, respectively, whose detailed definitions can be found in [22]. The quantities e^m and h^m are the electronic and magnetic column vectors containing the unknown coefficients in element m. The coefficients with a subscript f correspond to those on face f between element m and n. If the face f is on the excitation port, $\beta = 1$; or else, $\beta = 0$. Note here that the σ and $\overrightarrow{J_p}$ terms introduced in (4) are incorporated into (12).

Next, the fourth-order four-stage explicit Runge-Kutta method (ERK) is adopted by setting the operator $\mathcal{L}_i(u_n^i, t_n)$ equal to the right-hand side of (10), (11), and (12):

$$\begin{cases} k^{(1)} = \mathcal{L}_i(u_n^m, t_n) \\ k^{(2)} = \mathcal{L}_i\left(u_n^m + \frac{1}{2}\delta t\cdot k^{(1)}, t_n + \frac{1}{2}\delta t\right) \\ k^{(3)} = \mathcal{L}_i\left(u_n^m + \frac{1}{2}\delta t\cdot k^{(2)}, t_n + \frac{1}{2}\delta t\right) \\ k^{(4)} = \mathcal{L}_i\big(u_n^m + \delta t\cdot k^{(3)}, t_n + \delta t\big) \\ u_{t_{n+1}}^m = u_{t_n}^m + \frac{1}{6}\delta t\cdot\left(k^{(1)} + 2k^{(2)} + 2k^{(3)} + k^{(4)}\right) \end{cases}, \quad (13)$$

where $k^{(1-4)}$ are the partial terms associated with the ERK method, while $u_{t_n}^m$ represents the unknowns $e_{t_n}^m$, $h_{t_n}^m$, or $j_{t_n}^m$when solving for the electric field, magnetic field, or the polarization current vector at time step t_n, respectively. Also, δt is the maximum time-step size for the DGTD mesh, which is determined by the Courant-Freidrichs-Lewy (CFL) condition [16]. The physical time is equal to $t_n\delta t$.

It should be noted that (12) contains the term $\frac{de^m}{dt}$, which can be substituted with the right-hand side of (10). Therefore, it is efficient to arrange the iteration order to avoid redundant computation in the following way:

Step 1: Calculate $k_e^{(1)}$ and $k_h^{(1)}$ using (10) and (11).

Step 2: Calculate $k_j^{(1)}$ from (12) by setting $\frac{de^m}{dt} = k_e^{(1)}$ in Step 1.

Similarly, always calculate $k_e^{(m)}$ before $k_j^{(m)}$, and then calculate $k_j^{(m)}$ by setting $\frac{d\vec{E}}{dt} = k_e^{(m)}$, where m=1, 2, 3, 4.

III. NUMERICAL EXAMPLES

A. Reflection and transmission of a thin gold film

To validate the accuracy and convergence of the proposed DGTD + MDM method, we first studied a simple example in which a planewave propagates through a thin gold film upon normal incidence. The analytical results of the transmission and reflection can be derived from closed-formed Fresnel equations.

The gold film has a thickness of 5 nm. It is illuminated by a sinusoidally modulated Gaussian pulse. The transient response of the reflection and transmission coefficients is shown in Fig. 2 (a) with a mesh configuration consisting of prismatic elements. Through Fourier transformation, both the reflection and transmission coefficients can be recovered as shown in Fig. 2 (b). The results of the proposed DGTD + GDM algorithm match very well with the analytical data. As can be seen, a thin gold film becomes more transparent as the frequency increases, within the targeted spectral range.

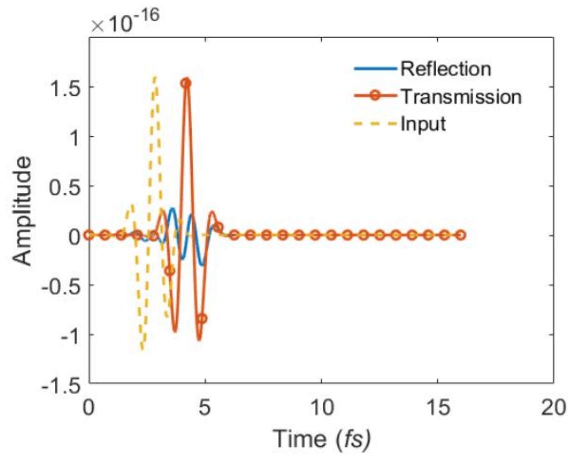

(a)

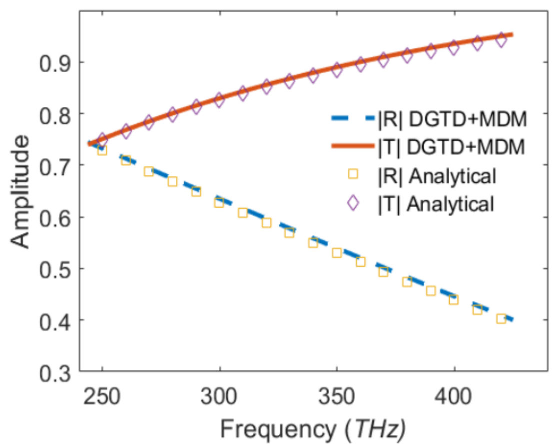

(b)

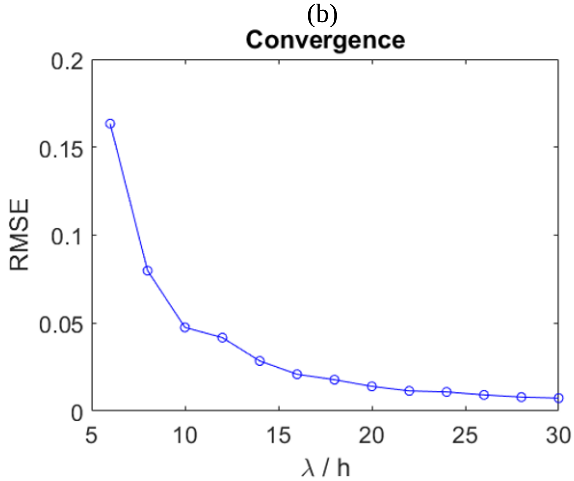

(c)

Fig. 2. Simulated results of the plane wave passing through a thin gold film. (a) The amplitude of the transient S-parameters. (b) Comparison of the frequency domain S-parameters from the prism-based DGTD with the modified Debye model and from the Fresnel equations. (c) Convergence plot showing accuracy improvement along with the refined mesh size.

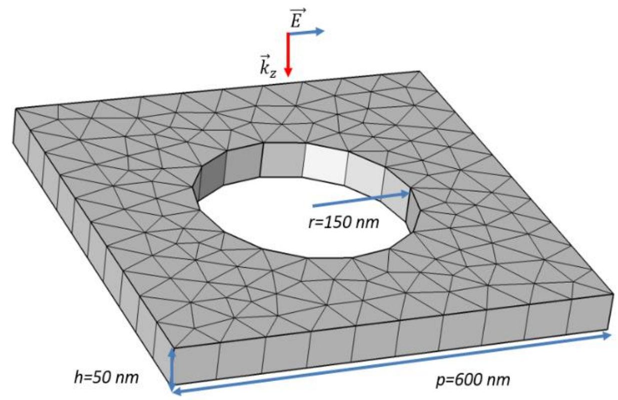

Fig. 3. Geometry of the unit cell of a gold nano-hole array frequency selective surface and its prismatic spatial discretization.

In order to investigate the accuracy of the proposed DGTD + GDM method, the relative errors of the numerical and analytical results are depicted as a function of the mesh size. Fig. 2 (c) shows the convergence plot which provides a means for quantifying the degree of accuracy improvement against refinements in the mesh. The algorithm was tested for different mesh sizes, where a measure of the accuracy was determined from the root mean square error (RMSE), which here is defined as:

$$RMSE = \sqrt{\frac{\sum_{1}^{N_f}(R/T^{DGTD+GDM} - R/T^{Analytical})^2}{N_f}}, \quad (14)$$

such that the performance was compared at N_f sampling frequencies. The convergence test was done with center frequency of 360 *THz*.

B. Illumination on a thin gold hole array

At this point we apply the prism-based DGTD method with the MDM to compute the S-parameters of a representative FSS structure for validation. Fig. 3 illustrates a single unit cell of the doubly periodic infinite FSS. The unit cell of the FSS under consideration contains a thin layer of a nano-hole array, where the gold film has a thickness of 50 nm. The 150 nm radius holes are spaced with a 600 nm lattice period [15]. Prismatic mesh cells represent the optimal discretization for such thin planar structures. The excitation of the normally incident field is modeled by a magnetic current with an amplitude corresponding to a sinusoidally modulated Gaussian pulse in order to generate a wideband response.

Figure 3 also depicts the prismatic spatial discretization utilized by the proposed algorithm. The minimum element length is about 34 nm, while the time step δt is set to 9.5 atto seconds. As can be seen, compared with a conventional tetrahedral mesh, the prismatic mesh represents the optimal choice for discretizing such planar structures.

S-parameters are a typically used metric to demonstrate the frequency dependent performance of an FSS. To extract the S-parameters, we expand the electric coefficient corresponding to the mode distribution at the input and output wave port j. The transient results generated by the prism-based DGTD with the modified Debye model are shown in Fig. 4 (a). A total of 6,000 time steps were computed, corresponding to nearly 58 femto-seconds. In order to demonstrate the frequency selective property, the transient S-parameters shown in Fig. 4 (a) are Fourier transformed to the frequency domain and plotted in Fig. 4 (b). For comparison, Fig. 4 (b) also contains the simulated result obtained from the commercial CST software package [28]. Since most commercial software packages, including CST, are not able to simulate MDM materials, the comparison was made with simulation results from CST's frequency domain solver (FEM) using imported experimental dispersion data [27]. Figure 4 (b) shows that the result of the proposed algorithm yields good agreement with CST. Some minor disagreement exists because of the difference between the frequency- and time-domain methods, as well as the discrepancy between the experimental material dispersion and the modified Debye fitting model. Moreover, the prism-based DGTD with the MDM algorithm requires only 45 seconds to perform the computations, while the CST software with default settings consumes 93 seconds, as shown in Table 1. This computational efficiency enhancement comes from the optimal spatial discretization enabled by prismatic elements, the first-order derivative modified Debye model, and the ease by which parallel computing can be utilized within the DGTD framework.

The gold nano-hole array demonstrates band-pass performance, with a remarkable transmission enhancement observed at 390 THz. As presented in [29], this type of extraordinary transmission behavior can be primarily attributed to the excitation of a surface plasmon at the metallic hole array structure interface. Concisely, the incident light couples into electromagnetic surface waves (i.e., surface plasmon polaritons (SPPs) at the metal-dielectric interface), which then radiate through reciprocal interactions with the structure. This, in turn, produces unique features in the transmission and reflection spectra. The numerical simulations were performed on a laptop with a 2.6 GHz Intel i6700HQ CPU, 4 cores, 8 threads, and 16 GB of memory. The algorithm has been fully parallelized with all 8 threads using OpenMP.

Table 1: Comparison of the number of elements, number of unknowns, CPU time, and memory consumption for different methods

Method	Tetra CST FEM + Exp	Prism DGTD + MDM
Number of Elements*	12,105	7,168
Number of Unknowns	79,344	193,536
CPU Times (s)	93	45
Memory (MB)	923	1,978

* For better comparison, the tetrahedral and prism meshes in this table have the same upper bound of mesh size (element length).

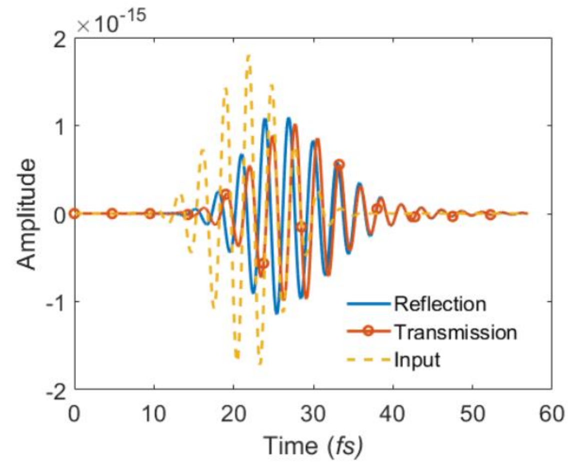

(a)

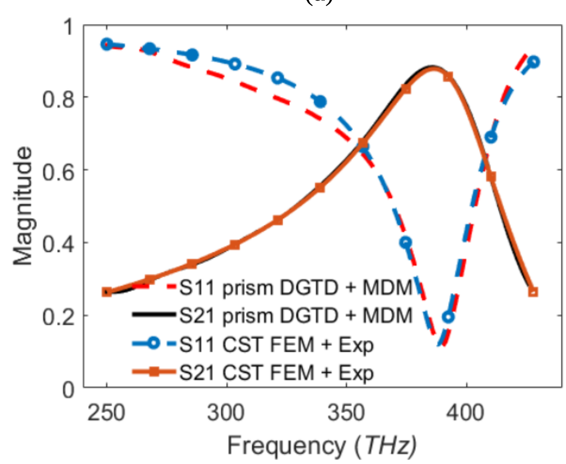

(b)

Fig. 4. Simulated results of the gold nano-hole array frequency selective surface. (a) The amplitude of the transient S-parameters. (b) Comparison of the frequency domain S-parameters from the prism-based DGTD with the modified Debye model (MDM) and from the *CST* FEM solver with imported experimental dispersive permittivity (Exp) [27].

IV. CONCLUSION

A prism-based DGTD algorithm together with a modified Debye model was proposed for simulating electromagnetic fields of planar metal structures (*e.g*., FSS and metasurfaces) that are dispersive in the optical spectrum. The ADE method and a high-order Runge-Kutta scheme were introduced as effective methodologies for integrating the modified Debye model into DGTD. The proposed algorithm was then used to simulate an FSS consisting of a gold film with a patterned nano-hole array, which was shown to exhibit enhanced transmission at a specific frequency in the optical regime due to the surface plasmatic effect. The extracted S-parameters agree well with the results produced by commercial software packages. Moreover, the DGTG formulation was found to be more efficient than the commercial solvers due to the prismatic elements, the first-order derivative modified Debye model, and the ability to readily exploit parallel computing architectures.

ACKNOWLEDGMENT

This work was supported in part by the Penn State MRSEC, Center for Nanoscale Science (NSF DMR-1420620), DARPA/DSO Extreme Optics and Imaging (EXTREME) Program (HR00111720032), National Science Foundation of China (61901132).

REFERENCES

[1] B. A. Munk, *Frequency Selective Surfaces: Theory and Design*. John Wiley & Sons, 2005.

[2] S. Mahashabde, A. S. Sobolev, M. A. Tarasov, G. E. Tsydynzhapov, and L. S. Kuzmin, "Planar frequency selective bolometric array at 350 GHz," *IEEE Transactions on Terahertz Science and Technology*, vol. 5, no. 1, pp. 37-43, Jan. 2015.

[3] T. Hong, W. Xing, Q. Zhao, Y. Gu, and S. Gong, "Single-layer frequency selective surface with angular stability property," *IEEE Antennas and Wireless Propagation Letters*, vol. 17, no. 4, pp. 547-550, Apr. 2018.

[4] F. Yang and Y. Rahmat-Samii, *Electromagnetic Band Gap Structures in Antenna Engineering*. Cambridge University Press, Cambridge, UK, 2009.

[5] B. A. Munk, *Metamaterials: Critique and Alternatives*. John Wiley & Sons, 2009.

[6] F. Capolino, *Theory and Phenomena of Metamaterials*. CRC Press, 2009.

[7] M. L. N. Chen, L. J. Jiang, and W. E. I. Sha, "Artificial perfect electric conductor-perfect magnetic conductor anisotropic metasurface for generating orbital angular momentum of microwave with nearly perfect conversion efficiency," *Journal of Applied Physics*, vol. 119, no. 6, p. 064506, Feb. 2016.

[8] X. Zheng, W. Smith, J. Jackson, B. Moran, H. Cui, D. Chen, J. Ye, N. Fang, N. Rodriguez, T. Weisgraber, and C. M. Spadaccini, "Multiscale metallic metamaterials," *Nat. Mater.*, vol. 15, no. 10, pp. 1100-1106, Oct. 2016.

[9] W. Mai, D. Zhu, Z. Gong, X. Lin, Y. Chen, J. Hu, and D. H. Werner, "Broadband transparent chiral mirrors: Design methodology and bandwidth analysis," *AIP Advances*, vol. 9, no. 4, p. 045305, Apr. 2019.

[10] K. S. Kunz, *The Finite Difference Time Domain Method for Electromagnetics*. CRC Press, 1993.

[11] A. Taflove, A. Oskooi, and S. G. Johnson, Eds., *Advances in FDTD Computational Electrodynamics: Photonics and Nanotechnology*. Boston: Artech House, 2013.

[12] J.-M. Jin, *The Finite Element Method in Electromagnetics*. Third edition, Hoboken, New Jersey: John Wiley & Sons Inc., 2014.

[13] S. D. Gedney, J. C. Young, T. C. Kramer, and J. A. Roden, "A discontinuous Galerkin finite element time-domain method modeling of dispersive media," *IEEE Transactions on Antennas and Propagation*, vol. 60, no. 4, pp. 1969-1977, Apr. 2012.

[14] Q. Ren, H. Bao, S. D. Campbell, L. J. Prokopeva, A. V. Kildishev, and D. H. Werner, "Continuous-discontinuous Galerkin time domain (CDGTD) method with generalized dispersive material (GDM) model for computational photonics," *Opt. Express*, vol. 26, no. 22, p. 29005, Oct. 2018.

[15] H. Bao, L. Kang, S. D. Campbell, and D. H. Werner, "Discontinuous Galerkin time domain analysis of electromagnetic scattering from dispersive periodic nanostructures at oblique incidence," *Opt. Express*, vol. 27, no. 9, p. 13116, Apr. 2019.

[16] W. Mai, J. Hu, P. Li, and H. Zhao, "An efficient and stable 2-D/3-D hybrid discontinuous Galerkin time-domain analysis with adaptive criterion for arbitrarily shaped antipads in dispersive parallel-plate pair," *IEEE Transactions on Microwave Theory and Techniques*, vol. 65, no. 10, pp. 3671-3681, Oct. 2017.

[17] W. Mai, P. Li, C. G. Li, M. Jiang, W. Hao, L. Jiang, and J. Hu, "A straightforward updating criterion for 2-D/3-D hybrid discontinuous Galerkin time-domain method controlling comparative error," *IEEE Transactions on Microwave Theory and Techniques*, vol. 66, no. 4, pp. 1713-1722, Apr. 2018.

[18] W. Mai, P. Li, H. Bao, X. Li, L. Jiang, J. Hu, and D. H. Werner, "Prism-based DGTD with a simplified periodic boundary condition to analyze FSS with D2n symmetry in a rectangular array under normal incidence," *IEEE Antennas and Wireless Propagation Letters*, vol. 18, no. 4, pp. 771-775, Apr. 2019.

[19] Q. Hong and J Kraus, "Uniformly stable discontinuous Galerkin discretization and robust iterative solution methods for the Brinkman problem," *SIAM J. Numer. Anal*., vol. 54, no. 5, pp. 2750-2274, Sep. 2006.
[20] S. P. Gao, Y. L. Lu, and Q. S. Cao, "Hybrid method combining DGTD and TDIE for wire antenna-dielectric interaction," *Applied Computational Electromagnetics Society Journal*, vol. 30, no. 6, 2015.
[21] L. Zhao, G. Chen, and W. Yu, "An efficient algorithm for SAR evaluation from anatomically realistic human head model using DGTD with hybrid meshes", *Applied Computational Electromagnetics Society Journal*, vol. 31, no. 6, 2016.
[22] W. Mai, S. D. Campbell, E. B. Whiting, L. Kang, P. L. Werner, Y. Chen, and D. H. Werner, "Prismatic discontinuous Galerkin time domain method with an integrated generalized dispersion model for efficient optical metasurface analysis," *Opt. Mater. Express*, vol. 10, pp. 2542-2559, 2020.
[23] J. T. Krug, E. J. Sánchez, and X. S. Xie, "Design of near-field optical probes with optimal field enhancement by finite difference time domain electromagnetic simulation," *J. Chem. Phys.*, vol. 116, no. 24, pp. 10895-10901, June 2002.
[24] E. X. Jin and X. Xu, "Plasmonic effects in near-field optical transmission enhancement through a single bowtie-shaped aperture," *Appl. Phys. B*, vol. 84, no. 1, pp. 3-9, July 2006.
[25] H. Gai, J. Wang, and Q. Tian, "Modified Debye model parameters of metals applicable for broad-band calculations," *Appl. Opt.*, vol. 46, no. 12, p. 2229, Apr. 2007.
[26] S. A. Maier, *Plasmonics: Fundamentals and Applications*. New York: Springer, 2007.
[27] E. D. Palik, *Handbook of Optical Constants of Solids*. Academic, p. 294, 1985.
[28] CST Microwave Studio, ver. 2008, Computer Simulation Technology, Framingham, MA, 2008.
[29] J. W. Yoon and R. Magnusson, "Fano resonance formula for lossy two-port systems," *Opt. Express*, vol. 21, no. 15, pp. 17751-17759, July 2013.

Wending Mai received the B.S. degree in Electronic Information Science and Technology, M.S. degree in Radio Physics, and Ph.D. degree in Electromagnetic and Microwave Technology from the University of Electronic Science and Technology of China, Chengdu, China, in 2007, 2010, and 2019 respectively.

In 2007, he was a Student Researcher in the Lenovo Research Institute, Chengdu. From 2010 to 2012, he was a Marketing Engineer in Texas Instruments Incorporated, Dallas, TX, USA. From 2013 to 2015, he was an Assistant Professor in Xichang College. From 2017 and 2019, he has been a Visiting Scholar and a Postdoc in the Computational Electromagnetics and Antennas Research Laboratory, The Pennsylvania State University, University Park, PA, USA. His current research interests include knot electromagnetics, computational electromagnetics, metamaterials and microwave imaging.

Mai is a Senior Member of the Institute of Electrical and Electronics Engineers (IEEE), a Member of the Applied Computational Electromagnetics Society (ACES), and a Member of the Institute of Physics (IOP). He is the recipient of the Excellent Student Paper Award presented by the IEEE Chengdu Section in 2017, and the Best Paper Award (ranked first) from the Chinese Journal of Radio Science in 2018.

Benjamin Zerbe graduated from Grove City College in 2017 with a bachelor's degree in Applied Physics and Computer Engineering and a minor in Computer Science. While there, he engaged in nano-fabrication and Casimir-Polder effect research under Dr. Jeffrey Wolinski. After graduation, he joined E x H, Inc. and worked on the GEMSIF electromagnetics design suite and its various solvers and optimization algorithms. He joined CEARL in 2020 and is currently working towards his Ph.D. in Electrical Engineering under the guidance of Prof. Douglas H. Werner.

His research interests include computational electromagnetics, computational physics, machine learning, metamaterials, optimization algorithms, and antenna design.

Douglas H. Werner received the B.S., M.S., and Ph.D. degrees in Electrical Engineering and the M.A. degree in Mathematics from The Pennsylvania State University (Penn State), University Park, PA, USA, in 1983, 1985, 1989, and 1986, respectively. He holds the John L. and Genevieve H. McCain Chair Professorship in the Department of Electrical Engineering, Penn State. He is the Director of the Computational Electromagnetics and Antennas Research Laboratory (CEARL: http://cearl.ee.psu.edu/) and a faculty member of the Materials Research Institute (MRI), Penn State. He holds 20 patents, has published over 900 technical articles and proceedings articles, and has authored 30 book chapters with several additional chapters currently in preparation. He has published several books, including Frontiers in Electromagnetics (Piscataway, NJ, USA: IEEE Press, 2000), Genetic Algorithms in Electromagnetics (Hoboken, NJ, USA: Wiley/IEEE, 2007), Transformation Electromagnetics and Metamaterials: Fundamental Principles and Applications (London, U.K.: Springer, 2014), Electromagnetics of Body Area Networks: Antennas, Propagation, and RF Systems (Hoboken: Wiley/IEEE, 2016), and Broadband Metamaterials in Electromagnetics: Technology and Applications (Pan Stanford Publishing, 2017). He has also contributed chapters for several books, including Electromagnetic Optimization by Genetic Algorithms (New York: Wiley Interscience, 1999), Soft Computing in Communications (New York: Springer, 2004), Antenna Engineering Handbook (New York: McGraw-Hill, 2007), Frontiers in Antennas: Next Generation Design and Engineering (New York: McGraw-Hill, 2011), Numerical Methods for Metamaterial Design (New York: Springer, 2013), Computational Electromagnetics (New York: Springer, 2014), Graphene Science Handbook: Nanostructure and Atomic Arrangement (Abingdon, Oxfordshire, U.K.: CRC Press, 2016), Handbook of Antenna Technologies (New York: Springer, 2016), and Transformation Wave Physics: Electromagnetics, Elastodynamics and Thermodynamics (Boca Raton, FL, USA: CRC Press, 2016). His research interests include computational electromagnetics (MoM, FEM, FEBI, FDTD, DGTD, CBFM, RCWA, GO, GTD/UTD), antenna theory and design, phased arrays (including ultrawideband arrays), microwave devices, wireless and personal communication systems (including body-area networks), wearable and e-textile antennas, RFID tag antennas, conformal antennas, reconfigurable antennas, frequency-selective surfaces, electromagnetic wave interactions with complex media, metamaterials, electromagnetic bandgap materials, zero and negative index materials, transformation optics, nanoscale electromagnetics (including nanoantennas), fractal and knot electrodynamics, and nature-inspired optimization techniques (genetic algorithms, clonal selection algorithms, particle swarm, wind-driven optimization, and various other evolutionary programming schemes). Werner is a fellow of the IEEE, IET, OSA, ACES, and the PIERS Electromagnetics Academy. He is also a Senior Member of the National Academy of Inventors (NAI) and SPIE. He was a recipient of the 1993 Applied Computational Electromagnetics Society (ACES) Best Paper Award, the 1993 International Union of Radio Science (URSI) Young Scientist Award, and the Pennsylvania State University Applied Research Laboratory Outstanding Publication Award in 1994. He has coauthored (with one of his graduate students) an article published in the IEEE Transactions on Antennas and Propagation which received the 2006 R. W. P. King Award. He also received the inaugural IEEE Antennas and Propagation Society Edward E. Altshuler Prize Paper Award, the Harold A. Wheeler Applications Prize Paper Award in 2011 and 2014, respectively, the DoD Ordnance Technology Consortium (DOTC) Outstanding Technical Achievement Award in 2018, the 2015 ACES Technical Achievement Award, the 2019 ACES Computational Electromagnetics Award, the IEEE Antennas and Propagation Society 2019 Chen-To Tai Distinguished Educator Award, the College of Engineering PSES Outstanding Research Award, the Outstanding Teaching Award in March 2000 and March 2002, respectively, and the PSES Premier Research Award in 2009. He was also presented with the IEEE Central Pennsylvania Section Millennium Medal. He is a former Associate Editor of Radio Science, a former Editor of the IEEE Antennas and Propagation Magazine, an Editorial Board Member of Scientific Reports (a Nature subjournal), an Editorial Board Member of EPJ Applied Metamaterials, an Editor of the IEEE Press Series on Electromagnetic Wave Theory and Applications, and a member of URSI Commissions B and G, Eta Kappa Nu, Tau Beta Pi, and Sigma Xi.